Magnetocaloric effect in in Tb60Ni30Al10 glass : a material that can either heat or cool upon magnetization

Stéphane Gorsse, Charlotte Mayer, Bernard Chevalier

Magnetocaloric effect in $Tb_{60}Ni_{30}Al_{10}$ glass: A material that can either heat or cool upon magnetization

S. Gorsse,[1,2,a)] C. Mayer,[1] and B. Chevalier[1]
[1]*CNRS, Université de Bordeaux, ICMCB, 87 avenue du Docteur Albert Schweitzer, 33608 Pessac Cedex, France*
[2]*IPB, ENSCPB, 16 avenue Pey-Berland, 33607 Pessac, France*

(Received 8 September 2010; accepted 12 December 2010; published online 9 February 2011)

The $Tb_{60}Ni_{30}Al_{10}$ amorphous alloy was prepared by melt-spinning in the form of ribbons. Its magnetic behavior shows upon magnetization the occurrence of a spin glass to ferromagnetic and a paramagnetic to ferromagnetic transitions at 5 and 48 K. The magnetocaloric effects associated with these transitions were investigated. Large positive and negative magnetic entropy changes upon magnetization have been observed in a temperature range interesting for gas liquefaction. © *2011 American Institute of Physics*. [doi:10.1063/1.3544450]

The magnetocaloric effect (MCE) is a temperature change in magnetic solids in a varying magnetic field.[1] It results of the coupling of the magnetic spins with the magnetic field and is related to a magnetic entropy change. As the compression of a gas, isothermal magnetization decreases the entropy and, in a reversible manner, adiabatic demagnetization, similarly to the expansion of a gas, restores the zero-field entropy by means of the thermal energy given by the phonons. This causes the material to cool. It is then possible to perform magnetically the cycle of a thermal machine. MCE is used for low-temperature cryogenic applications and is considered as an energy-efficient and environmentally-friendly refrigerant technology near room temperature thanks to the development of giant MCE materials ($\Delta S > 10$ J kg^{-1} K^{-1} and $\Delta T > 5$ K for $\Delta H = 2T$) in which the magnetic transition is associated with a first order transition.[2]

Some materials exhibit inverse MCE that is the cooling under magnetization.[3–9] This requires an increase in the magnetic entropy on application of a magnetic field. Inverse MCE occurs in system having less ordered magnetic transition such as antiferromagnetic/ferromagnetic (AF/FM), AF-collinear/AF-noncollinear, AF/ferrimagnetic or spin-glass/FM (SG/FM). The last situation can be found in rare earth (RE)-based metallic glasses when SG state arises from random magnetic anisotropy (RMA). On cooling, the ordered FM phase develops from the disordered PM state and reenters into another disordered SG phase. Some examples of such systems are Nd-, Tb-, Dy-, Ho-, and Er-based metallic glasses[3–5] but entropy change due to inverse MCE has not been characterized in RE-based metallic glasses.

Here we examine the magnetic field-induced entropy change related to both MCE and inverse MCE in $Tb_{60}Ni_{30}Al_{10}$ glass. Large direct MCE and inverse MCE have been obtained at 48 and 5 K, respectively, which make this glassy material an efficient and versatile candidate as cryogenic solid-refrigerant at two different working temperatures.

The alloy composition $Tb_{60}Ni_{30}Al_{10}$ was designed based on topologic and thermodynamic criteria described elsewhere[10] to ensure a good glass forming ability. The amorphous alloy was prepared by melting precisely weighted amounts of high purity elements Tb, Ni, and Al in a levitation furnace. Melting was performed several times to ensure a good homogeneity, in a water-cooled copper crucible, under a purified argon atmosphere. The amorphous ribbons of the as-cast alloy were obtained by single-roller melt-spinning technique with a copper wheel velocity between 25 and 30 m s^{-1} in a purified argon atmosphere.

Structural state of the melt-spun ribbons was examined by x-ray diffraction (XRD). dc magnetization measurements were performed using a superconducting quantum interface device magnetometer in the temperature range of 5–200 K and applied fields up to 4.6 T.

The XRD pattern of the $Tb_{60}Ni_{30}Al_{10}$ melt-spun ribbons is shown in Fig. 1. Only two broad diffraction peaks are observed at similar 2θ angles reported elsewhere for $Tb_{55}Co_{20}Al_{25}$ (Ref. 4) which indicates a fully amorphous state.

Plot of the ratio H/M (H is the applied field and M the magnetization) as a function of the temperature at $\mu_0 H = 0.1$ T (Fig. 2), shows that the behavior of the $Tb_{60}Al_{10}Ni_{30}$ glass follows a Curie-Weiss law for temperatures above 80

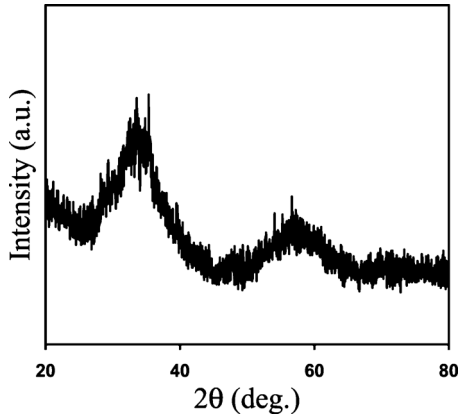

FIG. 1. XRD pattern of the melt-spun $Tb_{60}Ni_{30}Al_{10}$ ribbon.

a)Electronic mail: gorsse@icmcb-bordeaux.cnrs.fr.

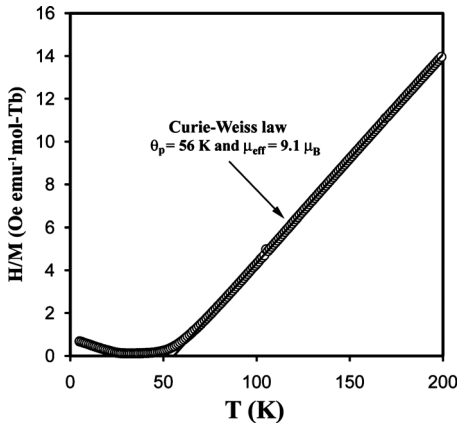

FIG. 2. H/M ratio plot of the $Tb_{60}Ni_{30}Al_{10}$ glass at $\mu_0 H=0.1$ T. The line represents the Curie–Weiss law at high temperature ($R^2=0.999$).

K, with a paramagnetic (PM) Curie temperature $\theta_P=56$ K and an effective moment of 9.1 μ_B/Tb. This value of the magnetic moment is close to the expected value of 9.72 μ_B for Tb^{3+} which suggests, together with the positive value of θ_P, a FM coupling between Tb^{3+} ions only.

Figure 3 presents the zero-field-cooling (ZFC) and field-cooling (FC) magnetization curves $M(T)$ of the amorphous alloy. The measurements are made in a low external field of $\mu_0 H=0.05$ T. In addition to the PM to FM transition observed for both the ZFC and FC magnetization curves at $T_C=48$ K (Curie temperature), the ZFC magnetization starts to decrease at $T_{irr}=38$ K (irreversibility temperature). Such bifurcation of the ZFC and FC curves at low temperature is generally observed in RE-based metallic glasses when the

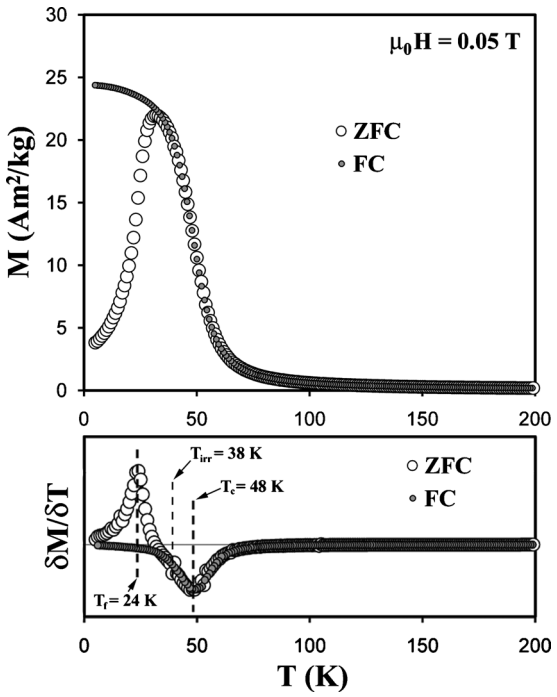

FIG. 3. Temperature dependence of the ZFC (open symbols) and FC (full symbols) magnetization curves at $\mu_0 H=0.05$ T for the $Tb_{60}Ni_{30}Al_{10}$ amorphous alloy. The bottom figure shows the derivative of the magnetization, $\partial M/\partial T$, vs T. T_f is the freezing temperature of the spins, T_{irr} is the irreversibility temperature between ZFC and FC curves and T_C the Curie temperature.

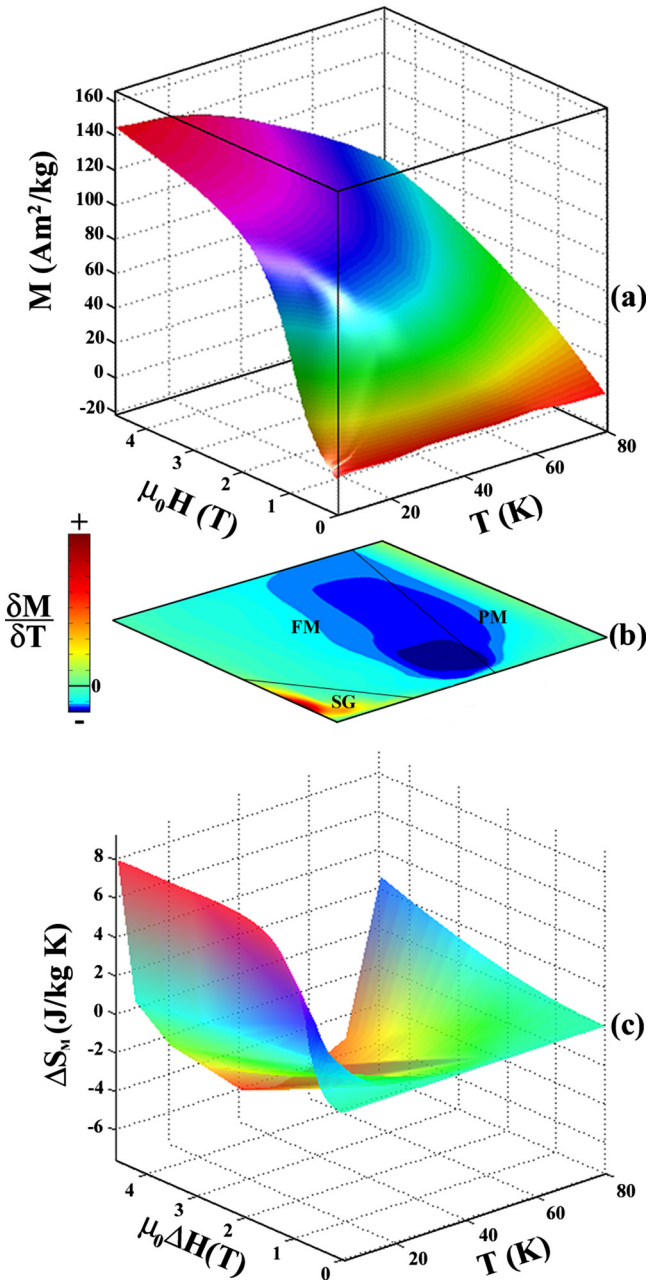

FIG. 4. (Color online) (a) Temperature and field dependence of the magnetization of the $Tb_{60}Ni_{30}Al_{10}$ amorphous alloy. The $M(H,T)$ surface is built from isothermal magnetization with increasing external field. (b) Projection of the derivative of $M(H,T)$ showing the SG, FM, and PM magnetic phase fields. (c) Related temperature and field dependences of the magnetic entropy change.

RE atom has an orbital moment (Nd-, Tb-, Dy-, Ho-, and Er-based glasses[3–5]) and not in Gd-based glasses ($L=0$).[11,12] It causes the presence of a temperature-dependent coercivity, and is interpreted as the random freezing of the magnetic moments along local anisotropy axes due to spin orbit coupling.[3] T_{irr} denotes the onset of the progressive freezing of spins toward randomly oriented axes—the FM phase starts to break up—and T_f (the freezing temperature), determined by the maximum of dM/dT, indicates the FM to SG transition below which the SG phase is fully developed at the expense of the FM phase.

Figure 4(a) shows the magnetization surface according

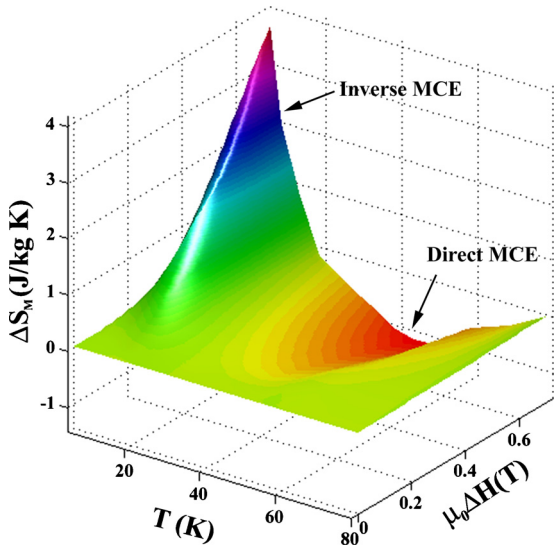

FIG. 5. (Color online) Zoom at low temperature and small applied field change in the magnetic entropy change showing both inverse and direct MCE in the $Tb_{60}Ni_{30}Al_{10}$ glass.

to the temperature and the external applied field obtained from isothermal $M(H)$ magnetization curves with a field increasing from 0 to 4.6 T at 5, 7, and 10 K and every 5 K between 10 and 80 K. The hysteretic behavior of $M(H,T)$ due to RMA can be visualized on the $M(H,T)$ surface by a change in its curvature in the low H-low T region. Even at 4.6 T, complete saturation is never achieved due to the progressive flipping of spins to a noncollinear FM alignment.[4]

The various SG, FM, and PM phase fields can be delimitated from the extremes of the derivative of $M(H,T)$ as seen in Fig. 4(b) which represents the projection of the $(dM/dT)_H$ surface on the (H,T) plan.

The resulting magnetocaloric response of the $Tb_{60}Ni_{30}Al_{10}$ amorphous alloy has been derived from Maxwell relation by integrating over the magnetic field:

$$\left(\frac{\partial S}{\partial M}\right)_T = \left(\frac{\partial M}{\partial T}\right)_H$$

where S represents the magnetic entropy.

The magnetic entropy change, ΔS_M, produced by the variation in a magnetic field from 0 to $H_{\max}$ is given by

$$\Delta S_M(T,H) = \int_0^{H_{\max}} \left(\frac{\partial M}{\partial T}\right)_H dH.$$

Figures 4(c) and 5 show the field and temperature dependence of the magnetic entropy change, $\Delta S_M(H,T)$. Since the sign of ΔS_M is determined by the sign of $\partial M/\partial T$, it is positive for temperature below T_{irr} and negative above. In the temperature range between 5 K and T_{irr} (T_{irr} ranges from 40 to ~5 K with increasing H), the application of an external magnetic field under adiabatic condition causes the alloy to cool ($\Delta S_M > 0$, MCE inverse) while it heats up if the magnetic field is applied above T_{irr} ($\Delta S_M < 0$, MCE). The inverse MCE of the sample is related to the SG/FM transition experienced by the alloy when applying the magnetic field at low T, and the direct MCE is due to the PM/FM transition.

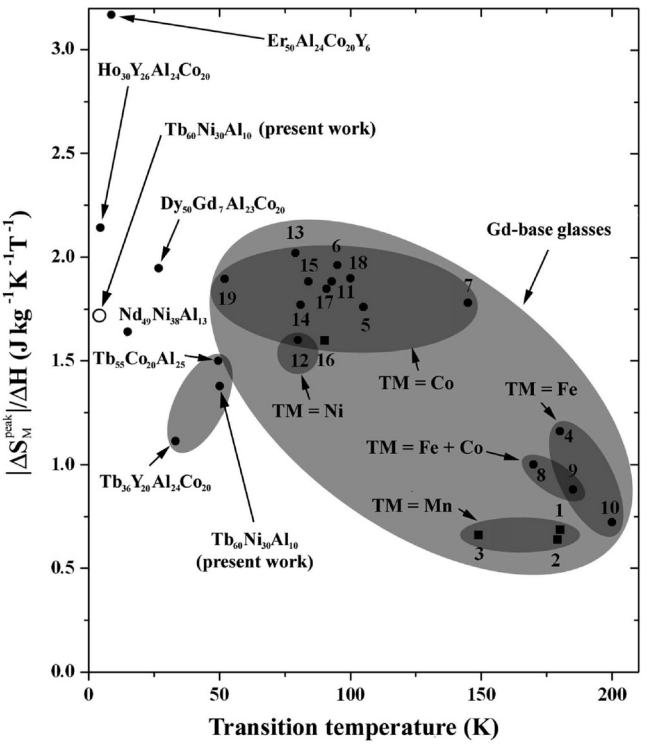

FIG. 6. Absolute values of the magnetic entropy change per field unit (4.6 or 5 T depending of the studies) vs the magnetic transition temperature of several amorphous RE-based metallic glasses. TM stands for the transition metal entering in the glass composition. For the $Tb_{60}Ni_{30}Al_{10}$ glass, open symbol is related to inverse MCE and plain symbol to direct MCE. Compounds legend: $Nd_{49}Ni_{38}Al_{13}$ (Ref. 3), $Tb_{55}Co_{20}Al_{25}$ (Ref. 4), $Tb_{36}Y_{20}Al_{24}Co_{20}$ (Ref. 9), $Dy_{50}Gd_7Al_{23}Co_{20}$ (Ref. 5), $Ho_{30}Y_{26}Al_{24}Co_{20}$ (Ref. 5), $Er_{50}Al_{24}Co_{20}Y_6$ (Ref. 5), 1—$Gd_{60}Mn_{30}In_{10}$ (Ref. 12), 2—$Gd_{60}Mn_{30}Ga_{10}$ (Ref. 12), 3—$Gd_{60}Mn_{30}Al_{10}$ (Ref. 12), 4—$Gd_{65}Fe_{20}Al_{15}$ (Ref. 15), 5—$Gd_{55}Co_{20}Al_{25}$ (Ref. 16), 6—$Gd_{52.5}Co_{16.5}Al_{31}$ (Ref. 17), 7—$Gd_{60}Co_{30}Al_{10}$ (Ref. 18), 8—$Gd_{60}Fe_{10}Co_{20}Al_{10}$ (Ref. 18), 9—$Gd_{60}Fe_{20}Co_{10}Al_{10}$ (Ref. 18), 10—$Gd_{60}Fe_{30}Al_{10}$ (Ref. 18), 11—$Gd_{53}Al_{24}Co_{20}Zr_3$ (Ref. 19), 12—$Gd_{55}Ni_{25}Al_{20}$ (Ref. 16), 13—$Gd_{60}Co_{26}Al_{14}$ (Ref. 20), 14—$Gd_{51}Al_{24}Co_{20}Ce_5$ (Ref. 21), 15—$Gd_{48}Al_{25}Co_{20}Zr_3Er_4$ (Ref. 21), 16—$Gd_{51}Al_{24}Co_{20}Nb_1B_4$ (Ref. 21), 17—$Gd_{51}Al_{24}Co_{20}Zr_4Nb_1$ (Ref. 21), 18—$Gd_{51}Al_{24}Co_{20}Nb_1Cr_4$ (Ref. 21), 19—$Gd_{33}Er_{22}Al_{25}Co_{20}$ (Ref. 19).

The peak value of ΔS_M for the MCE at T_C=48 K is about −2.0 J kg^{-1} K^{-1} and −6.5 J kg^{-1} K^{-1} for a magnetic field change of 2 T and 4.6 T, respectively. These values compare well with others RE-based glasses and follow the global trend regarding the inverse relationship between ΔS_M and T_C (Fig. 6). The temperature range corresponding to the full-width at half maximum of the MCE entropy peak is 45 K and 50 K in field change of 2 and 4.6 T. Such broad peak of $\Delta S_M(T)$ is usual for magnetic amorphous alloys,[5,11–14] in contrast with crystalline materials that exhibit higher ΔS_M^{Peak} with narrower temperature range.[14] Lowering of T_C and broadening of ΔS_M are two general characteristics of amorphization.

The maximum of the magnetic entropy change due to inverse MCE at $T=T_f$ (<30 K) is about 3.7 J kg^{-1} K^{-1} and 8.0 J kg^{-1} K^{-1} for a magnetic field change of 0.6 T and 4.6 T, respectively, which is higher than the absolute value of MCE for this material at 48 K and those of Gd-based glasses (Fig. 6).

In conclusion, large MCE and inverse MCE are observed in the $Tb_{60}Ni_{30}Al_{10}$ in the temperature range of 5–50 K. In

addition to the coexistence of positive and negative MCE, others attractive features common to all metallic glasses such as the tunable nature of T_C, the small magnetic hysteresis loss, the high mechanical strength, the high oxidation, and corrosion resistances, and the polymerlike thermoplastic behavior, make the $Tb_{60}Ni_{30}Al_{10}$ amorphous alloy an interesting candidate as a solid refrigerant for gas liquefaction.

This work was supported by the Conseil Régional d'Aquitaine.

[1]E. Warburg, Ann. Phys. **249**, 141 (1881).
[2]V. K. Pecharsky and K. A. Gschneider, Phys. Rev. Lett. **78**, 4494 (1997).
[3]S. Gorsse, G. Orveillon, and B. Chevalier, J. Appl. Phys. **103**, 044902 (2008).
[4]J. Du, Q. Zheng, E. Bruck, K. H. J. Buschow, W. B. Cui, W. J. Feng, and Z. D. Zhang, J. Magn. Magn. Mater. **321**, 413 (2009).
[5]Q. Luo, D. Q. Zhao, M. X. Pan, and W. H. Wang, Appl. Phys. Lett. **90**, 211903 (2007).
[6]D. H. Wang, C. L. Zhang, H. C. Xuan, Z. D. Han, J. R. Zhang, S. L. Tang, B. X. Gu, and Y. W. Du, J. Appl. Phys. **102**, 013909 (2007).
[7]V. Franco, K. Pirota, V. Prida, A. Neto, A. Conde, M. Knobel, B. Hernando, and M. Vazquez, Phys. Rev. B **77**, 104434 (2008).
[8]S. Gorsse, B. Chevalier, S. Tuncel, and R. Pöttgen, J. Solid State Chem. **182**, 948 (2009).
[9]T. Krenke, E. Duman, M. Acet, E. F. Wassermann, X. Moya, L. Manosa, and A. Planes, Nature Mater. **4**, 450 (2005).
[10]G. Orveillon, O. N. Senkov, J.-L. Soubeyroux, B. Chevalier, and S. Gorsse, Adv. Eng. Mater. **9**, 483 (2007).
[11]S. Gorsse, B. Chevalier, and G. Orveillon, Appl. Phys. Lett. **92**, 122501 (2008).
[12]C. Mayer, B. Chevalier, and S. Gorsse, J. Alloys Compd. **507**, 370 (2010).
[13]Q. Luo and W. Wang, J. Non-Cryst. Solids **355**, 759 (2009).
[14]S. Tence, S. Gorsse, E. Gaudin, and B. Chevalier, Intermetallics **17**, 115 (2009).
[15]Q. Y. Dong, B. G. Shen, J. Chen, J. Shen, F. Wang, H. W. Zhang, and J. R. Sun, J. Appl. Phys. **105**, 053908 (2009).
[16]J. Du, Q. Zheng, Y. B. Li, Q. Zhang, D. Li, and Z. D. Zhang, J. Appl. Phys. **103**, 023918 (2008).
[17]H. Fu, M. S. Guo, H. J. Yu, and X. T. Zu, J. Magn. Magn. Mater. **321**, 3342 (2009).
[18]B. Schwarz, B. Podmiljsak, N. Mattern, and J. Eckert, J. Magn. Magn. Mater. **322**, 2298 (2010).
[19]Q. Luo, Q. Zhao, M. X. Pan, and W. H. Wang, Appl. Phys. Lett. **89**, 081914 (2006).
[20]H. Fu, X. Y. Zhang, H. J. Yu, B. H. Teng, and X. T. Zu, Solid State Commun. **145**, 15 (2008).
[21]Q. Luo and W. H. Wang, J. Alloys Compd. **495**, 209 (2010).